IOP PUBLISHING JOURNAL OF PHYSICS: CONDENSED MATTER

J. Phys.: Condens. Matter **19** (2007) 136209 (11pp) doi:10.1088/0953-8984/19/13/136209

Swift heavy ion irradiation of MgB_2 thin films: a comparison between gold and silver ion irradiations

Himanshu Narayan[1,3], Ravindra K Bhatt[2], H M Agrawal[2], R P S Kushwaha[2] and H Kishan[1]

[1] Superconductivity Division, National Physical Laboratory, Dr K S Krishnan Marg, New Delhi 110012, India
[2] Department of Physics, G B Pant University of Agriculture and Technology, Pantnagar 263145, India

E-mail: h.narayan@nul.ls

Received 7 December 2006, in final form 12 February 2007
Published 13 March 2007
Online at stacks.iop.org/JPhysCM/19/136209

Abstract

The effect of 200 MeV Au ion irradiation on the temperature and field dependence of the critical current density, J_c, of MgB_2 thin films on sapphire substrates is reported. The results have been presented in comparison with those obtained after 200 MeV Ag ion irradiation of a similar film. After irradiation, the critical temperature T_c decreased for all samples except for the one with a higher dose of gold ions, where it increased marginally. This observation was also confirmed from measurements of magnetization as a function of temperature with a constant applied field of 10^{-2} T. The critical current density, J_c, was estimated from the widths of magnetization loops using Bean's critical state model. It has been found that J_c increases after irradiation, the enhancement being more pronounced for the Au ion irradiation. The higher enhancement of J_c by Au ion irradiation may be attributed to higher flux-pinning efficiency of the irradiated samples. It has been concluded that, although the flux-line shear (FLS) model satisfactorily explains the silver ion irradiation induced enhancement of J_c, some other mechanisms also seem to play a role in the J_c enhancement by gold ion irradiation.

1. Introduction

Superconductivity at 40 K was discovered in magnesium diboride (MgB_2) [1] only in the year 2001, although this material has been known since 1952. Soon after this discovery, a number of groups all over the world switched their interests toward the investigation of its unusual superconducting properties, such as high critical current density (J_c), large coherence

[3] Author to whom any correspondence should be addressed. Present address: Department of Physics and Electronics, National University of Lesotho, Roma 180, Lesotho, Southern Africa.

Table 1. Irradiation parameters.

Ions	Energy E (10^6 eV)	Electronic energy loss S_e (keV nm^{-1})	Projected range R_p (10^{-6} m)	Irradiated thin films
^{197}Au	200	21.85	15.18	Set 1
^{107}Ag	200	15.67	17.86	Set 2

length (χ) [2] and the absence of weak links across grain boundaries (GB) [3]. Some of these properties were very promising as far as the technical exploitation of the material was concerned. Therefore, efforts were made to enhance its useful properties by various available methods. Since, for high-temperature superconducting cuprates (HTSC), it is well established that swift heavy ion (SHI) irradiation enhances J_c significantly at the cost of a slight decrease in T_c, this method has also been employed by various groups.

The first irradiation experiment on MgB_2 fragments was performed almost immediately after the discovery of superconductivity in this material [4]. An enhancement of J_c was observed after 2 MeV proton irradiation. Very soon, many other groups got involved in the ion irradiation experiments, using all available forms of MgB_2 and various ion-energy combinations. In the process, for example, MgB_2 was subjected to particle beams such as electrons [5] and neutrons [6] as well as to SHI irradiations using helium [7], silver [8–10], silicon and gold [11], lead [12], and uranium [13] beams. The results obtained were of mixed type, and moderate to significant enhancement of J_c as well as marginal improvement to severe degradation of T_c were reported. However, even after more than five years since the discovery of superconductivity in MgB_2, the need for a comprehensive understanding of the SHI beams' interactions with the material still persists.

In this paper we present the modification of the superconducting properties of MgB_2 thin films subjected to 200 MeV ^{197}Au ions and compare the results with those induced by 200 MeV ^{107}Ag ion irradiation in a similar film.

2. Experimental details

High-quality MgB_2 thin films, prepared by hybrid physical chemical vapour deposition on sapphire substrate, were procured from Superconix Inc. (USA) (for details about the preparation of MgB_2 thin films by this technique, see [14], for example). The film thickness was about 350 nm. Before irradiation, the films were characterized by x-ray diffraction, which ensured good sample quality. Scanning electron microscopy (SEM) was carried out before and after irradiation to verify the changes in microstructure. A Monte Carlo SRIM (stopping and range of ions in matter) program [15] was used to choose the ion-energy combinations for irradiation of the films in such a way that no implantation takes place.

Irradiation was carried out at the Materials Science Beam Line at IUAC, New Delhi, India using the 14 MV Pelletron accelerator facility. Two samples with dimensions of about 5.0 mm × 5.0 mm (hereafter called set 1) were irradiated by a 200 MeV ^{197}Au beam up to 5×10^{10} and 1×10^{12} ions cm^{-2}. Two other samples with dimensions of about 4.5 mm × 5.0 mm (hereafter called set 2) and almost identical properties to those of set 1 (in terms of grain size, crystallinity and resistivity behaviour) were irradiated under similar irradiation conditions by 200 MeV ^{107}Ag ions up to fluences of 1×10^{11} and 1×10^{12} ions cm^{-2}. In both cases, uniform irradiation of the samples was ensured by making the ion beam incident normally on the samples, scanning an area of about 7.0 mm × 7.0 mm. The details of the irradiation parameters are presented in table 1.

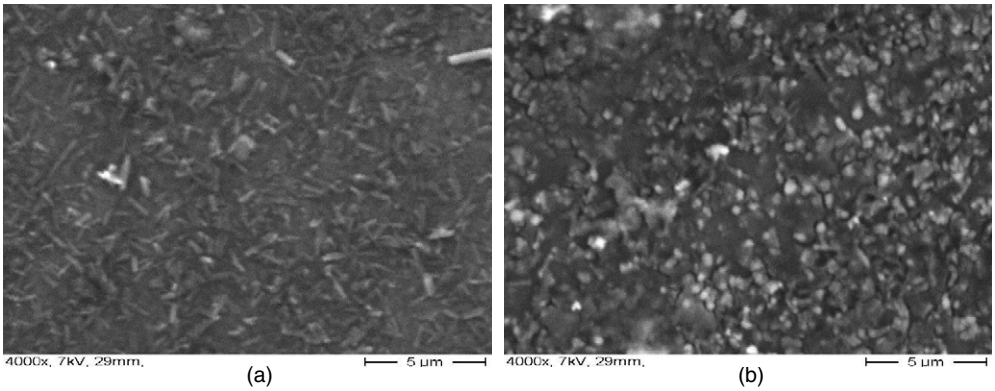

Figure 1. SEM picture of MgB_2 thin films at 4000×: (a) pristine; (b) irradiated with 200 MeV Au ions (1×10^{12} ions cm^{-2}).

The standard four-point probe technique in conjunction with a closed-cycle refrigerator setup was employed for transport measurements in the temperature range 20–300 K. For making contacts, good-quality copper wires and silver paste were used. A constant current of 100 μA was supplied from a programmable constant-current source through the outer probes, and the voltage developed across the inner two probes was measured using a digital voltmeter. The $R(T)$ data was collected using an automatic data acquisition system attached to the setup. Magnetic measurements of both the pristine and irradiated samples were carried out using a Quantum Design superconducting quantum interference device (SQUID) magnetometer. The magnetization M was measured as both a function of temperature T (in the range 5–60 K) as well as a function of the applied field B (from 0 to 3.5 T).

3. Results and discussion

Figure 1 depicts typical SEM images of the MgB_2 thin-film samples. In figure 1(a), for the pristine sample, elongated grains about 1.0 μm in size may clearly be seen uniformly distributed over a nearly homogeneous background. After both types of irradiation, the grains change their shape and size. For example, an SEM picture of the sample irradiated with a higher dose of Au ions is shown in figure 1(b). A comparison between these two pictures immediately reveals the irradiation-induced modification of the microstructure. The elongated shape of the grains seems to have changed after irradiation into small bead-shaped grains (with an average size of about 0.7 μm) spread over a background of tile-shaped structure (with an average tile size of about 4.0 μm). It is also noteworthy that the number and size of the bead-shaped grains decreases at higher dose, indicating that probably the elongated grains of the pristine samples first melt to form the bead-shaped grains, which further melt at higher irradiation doses and merge with the background.

Figure 2 shows the resistivity data as a function of temperature for both sets of samples. It is evident from this figure that the critical temperatures T_c for the pristine samples are 35.4 and 36.0 K for set 1 and set 2, respectively. It may be noted that these values are not optimum for both sets. To understand this variation in T_c, several reasons have been proposed, such as disorder at Mg sites, the formation of Mg vacancies, the presence of impurities and the oxidation of Mg. However, a sharp transition ($\Delta T_c \sim 1$ K) shows good grain connectivity of the pristine films. Also, the nature of the temperature dependence of resistivity of these

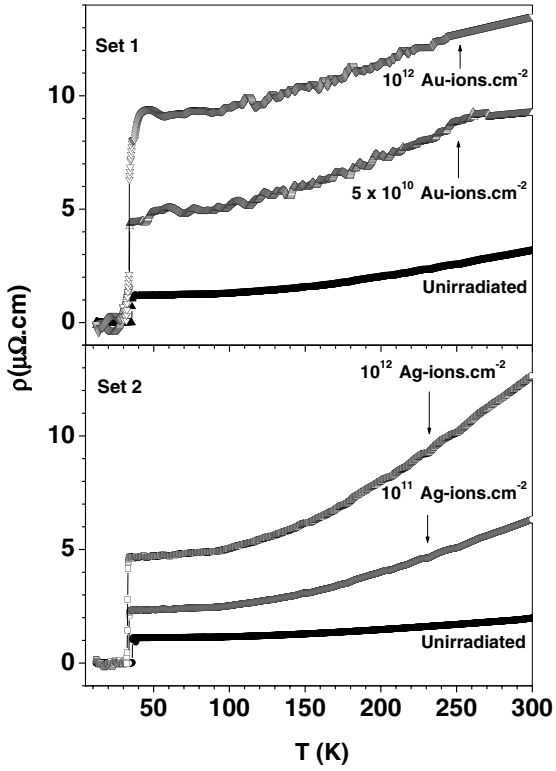

Figure 2. Resistivity as a function of temperature for both sets of samples.

Table 2. Data obtained from $R(T)$ plot.

Sample	Irradiation (ions cm^{-2})	T_c (K)	ρ_{40} (10^{-6} Ω cm)	$\Delta\rho$ (10^{-6} Ω cm)
Set 1, film 1	Pristine	35.4	1.17	1.99
Set 1, film 2	5×10^{10} Au	33.9	4.43	4.82
Set 1, film 3	1×10^{12} Au	35.9	8.92	4.58
Set 2, film 1	Pristine	36.0	1.12	0.87
Set 2, film 2	1×10^{11} Ag	33.9	2.33	3.99
Set 2, film 3	1×10^{12} Ag	32.5	4.66	7.99

samples is almost identical, except for the fact that the pristine sample of set 1 has slightly higher room-temperature resistivity compared to that of set 2.

The normalized magnetization data as a function of temperature $M(T)$, for a constant applied field of 1×10^{-2} T, is shown in figure 3. As expected, all the samples show a diamagnetic transition in the zero field cooled (ZFC) measurements. No significant diamagnetic signals were obtained in the field cooled (FC) measurement (shown only for the pristine samples of both sets, for clarity). The critical temperatures T_c, defined by the onset of transition, for the pristine samples were 35.4 and 36.0 K for set 1 and set 2, respectively. After irradiation, for the samples of set 1, T_c degraded to 33.9 K for a dose of 5×10^{10} Au ions cm^{-2}, whereas it unexpectedly improved slightly to 35.9 K for a dose of 1×10^{12} Au ions cm^{-2}. On the other hand, the T_c for samples of set 2 degraded to 33.9 and 32.5 K for doses of 1×10^{11} and

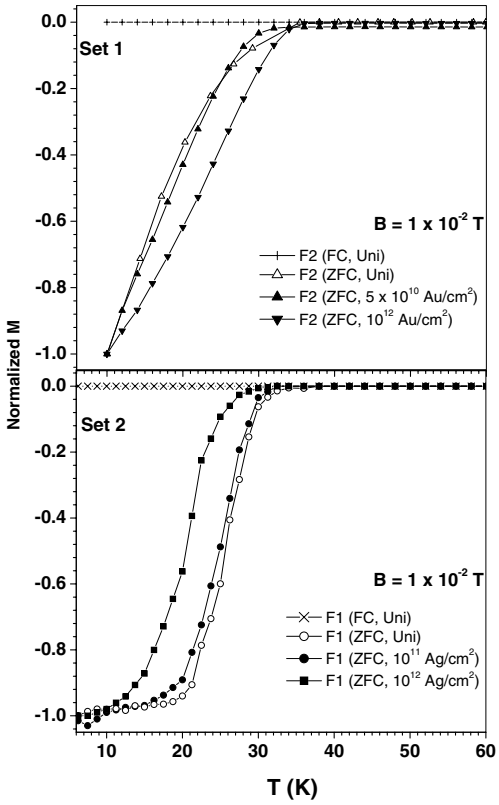

Figure 3. Normalized magnetization as a function of temperature at a constant applied field of 10^{-2} T for both sets of samples.

1×10^{12} Ag ions cm^{-2}, respectively. All these values of T_c are consistent with those obtained from the $R(T)$ data shown in figure 2.

Clear and marked differences are evident in the $R(T)$ curves for the irradiated samples as shown in figure 2. First, as expected, one can note the degradation of T_c after irradiation in all but one irradiated sample, although there is no systematic relationship between the ion dose and the change in T_c. Second, a higher dose of Au ion irradiation seems to introduce a wider transition broadening in the samples of set 1, whereas Ag ion irradiation does not lead to any significant change in the transition broadening in the samples of set 2. Moreover, the $R(T)$ data corresponding to Au ion irradiation does not seem to follow the same smooth trend as that of the pristine data, rather it shows some fluctuations. These fluctuations may be attributed to the possible irradiation-induced introduction of regions with slightly varying $R(T)$ properties (due to varying grain connectivity) in the wake of higher electronic energy loss (S_e). It is pertinent to note here that the slight improvement of T_c in the sample with a higher dose of Au ions may also be due to the contribution of regions with better grain connectivity.

The absolute value of resistivity at 40 K (ρ_{40}) and $\Delta\rho$ ($= \rho_{300} - \rho_{40}$) have been determined from the resistivity data and are summarized in table 2. It may easily be noted that the value of ρ_{40} increases with dose for both types of irradiation. The value of $\Delta\rho$ also increases with dose except for the sample irradiated with a higher dose of Au ions. An increase in $\Delta\rho$ after irradiation indicates a decrease in inter-grain connectivity [16]. From the calculated values of

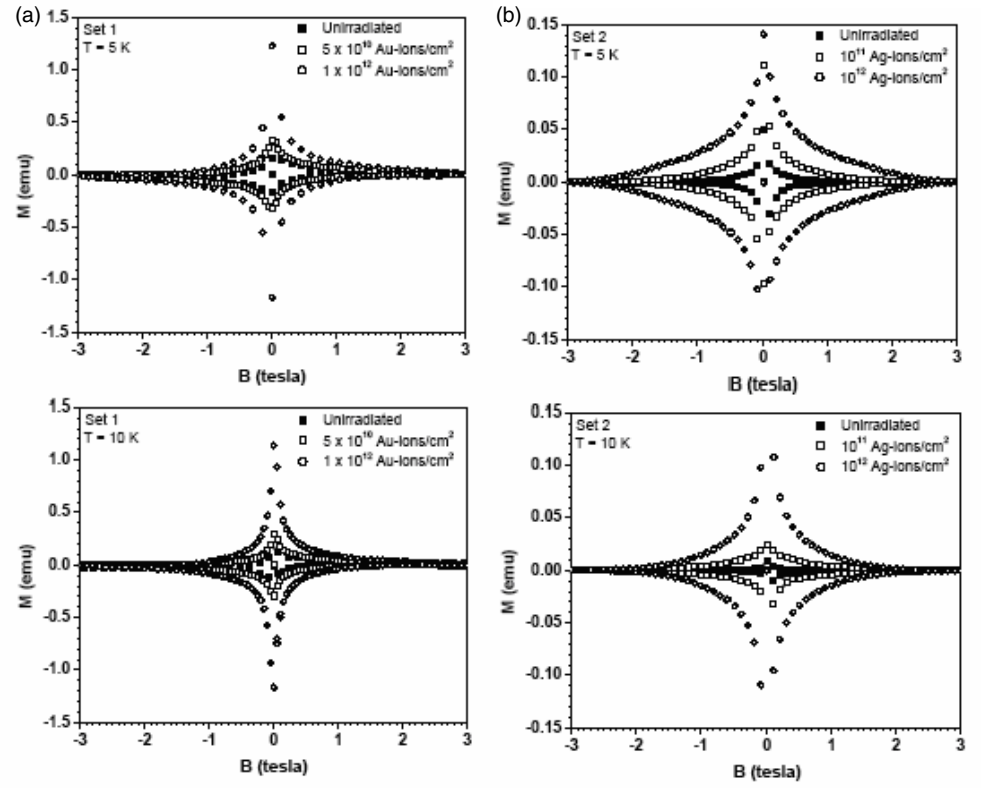

Figure 4. Magnetization loops measured at two different temperatures for both sets of samples.

$\Delta\rho$, it is evident that the inter-grain connectivity of the samples has definitely decreased after Ag ion irradiation (set 2). However, in set 1, after Au ion irradiation, the overall connectivity first decreased (for a dose of 5×10^{10} Au ions cm^{-2}) then probably increased slightly (for a dose of 1×10^{12} Au ions cm^{-2}). Although, in most cases, after irradiation a degradation of T_c is expected, some authors have also reported a marginal increase in T_c due to irradiation [17]. For the sample irradiated with a higher dose of Au ions, the slight increase in T_c may be associated with the possible improvement of grain connectivity due to irradiation, as evidenced by the small decrease in $\Delta\rho$ obtained from the resistivity data (see table 2). It is well established that almost all SHI-irradiation-induced effects are closely related to the S_e of incident ions in the target material. The type and amount of damage induced by irradiation also depend on the S_e value. At sufficiently large S_e, a high dose of irradiation may lead to large-scale atomic rearrangements in the target material. This has been reported for MgB_2 thin films too [9]. Since the S_e corresponding to 200 MeV Au ion irradiation of MgB_2 is quite high (see table 1), it seems plausible that, at an irradiation dose of 1×10^{12} ions cm^{-2}, atomic rearrangements have taken place in the sample, resulting in better grain connectivity, at least in some regions if not all over, and therefore there is a slight improvement in T_c. The irradiation-induced atomic rearrangement is supported by the SEM pictures too (see figure 1). Nevertheless, this observation definitely needs further investigation.

Figure 4(a) shows the M–B loops for samples of set 1 at constant temperatures of 5 and 10 K, respectively. It is evident from the figures that the loops are larger for a lower

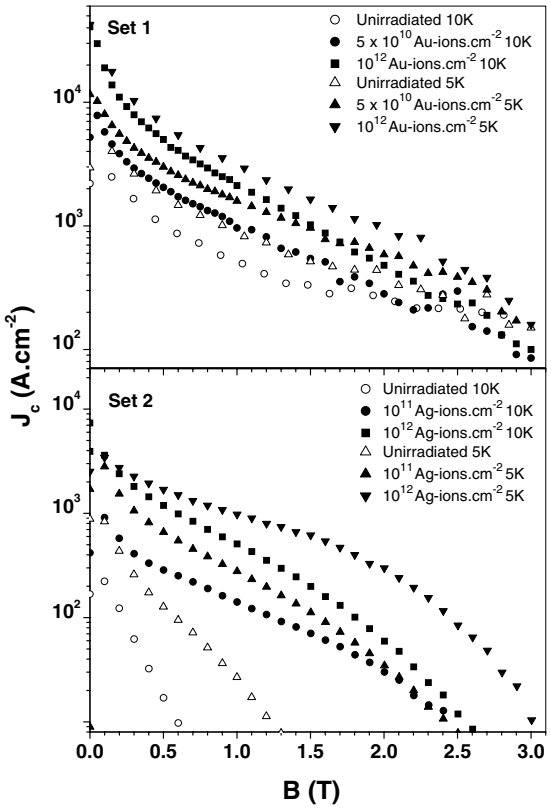

Figure 5. Critical current density as a function of applied field for both sets of samples at two different temperatures.

temperature and a higher dose of irradiation. This feature is present also in the M–B loops plotted in figure 4(b) for samples of set 2 at constant temperatures of 5 and 10 K, respectively. However, a comparison between figures 4(a) and (b) reveals that the loops corresponding to Au ion irradiation (set 1) are larger than those for Ag ion irradiation (set 2) by approximately an order of magnitude (compare the scales of the M axes in the two figures). In terms of the critical current density J_c, this means that Au ion irradiation leads to a larger enhancement of J_c compared to Ag ion irradiation. To show this observation clearly, the J_c values estimated using Bean's critical state model [18] from the M–B loops of figures 4(a) and (b) have been plotted in figure 5. According to Bean's model, J_c is related to the width of the magnetization loops by the formula $J_c = 30\Delta M/r$, where r is the radius corresponding to the total surface area of the sample, calculated from $\pi r^2 = xy$, x and y being the length and breadth of the film, respectively [19] ($x = y = 3.0$ mm for all samples used for magnetic measurements).

In figure 5, as expected, J_c shows the decreasing trend with increasing values of temperature and applied magnetic field. Also, an enhancement in J_c after irradiation is obvious for both sets of samples. However, this enhancement is more pronounced in the case of Au ion irradiation in comparison with the Ag ion irradiation. For example, at $T = 5$ K, for $B = 0$ T, J_c is increased by an order of magnitude, from about 6.1×10^3 to 6.2×10^4 A cm^{-2}, for a fluence of 1×10^{12} Au ions cm^{-2} in set 1. For the same values of temperature, applied field and dose, however, it is enhanced by a factor of seven, from about 1.1×10^3 to 7.7×10^3 A cm^{-2} in set

2 (Ag ion irradiation). Similarly, corresponding to $T = 10$ K and keeping other parameters unchanged, J_c increased from about 3.6×10^3 to 4.3×10^4 A cm^{-2} and from about 4.4×10^2 to 3.9×10^3 A cm^{-2} for Au and Ag ion irradiation, respectively.

It may also be noted from figure 5 that the value of $J_c(B)$ is about 10^2 A cm^{-2} at around $B = 3$ T, for all curves of set 1, and also that the $J_c(B)$ does not seem to tend to zero until a higher value of B is applied. This implies that the irreversibility field B_{irr} is higher than 3 T for both the pristine samples as well as the Au ion irradiated samples of set 1 (at both temperatures). On the other hand, in set 2, the value of $J_c(B)$ is about 10 A cm^{-2} (at 5 K) for the sample irradiated with 1×10^{12} Ag ions cm^{-2}. Further, the $J_c(B)$ in this curve tends to zero rather steeply at around $B = 3$ T. For all the other curves of this set, the $J_c(B)$ becomes zero at $B_{irr} < 3$ T. Interestingly, unlike the pristine sample of set 1, where B_{irr} is higher than 3 T for both the temperatures considered, that of set 2 shows $B_{irr} \approx 1.3$ and 0.6 T for the temperatures 5 and 10 K, respectively. This shows that the magnetic properties of the pristine samples of both sets were quite different. Obviously, these pristine magnetic properties should have partly affected the J_c enhancement after irradiation.

The enhancement of J_c by different magnitudes after the two irradiations may also be attributed to corresponding S_e values. At sufficiently higher values of S_e, columnar ion tracks are the expected form of damage. It has already been reported that 200 MeV Ag ions create ion tracks in polycrystalline bulk MgB_2 [8]. Obviously, 200 MeV Au ion irradiation should also lead to the formation of tracks because of an S_e value that is higher than that for Ag ions (see table 1). However, the size and the properties of the material within the tracks produced by the two irradiations may be entirely different. This should naturally be reflected in their flux-pinning efficiencies, thus leading to the observed difference in J_c enhancement.

In order to explain the possible difference between pinning mechanisms involved in the two sets, we now discuss the results in the light of the flux-line shear (FLS) model [20]. This model assumes that weaker superconducting regions (e.g. the grain boundaries [17] and/or small precipitates [21]) can allow the flux lines to shear flow when some strong pinning centres (e.g. the columnar tracks produced by irradiation) are present in the sample. The volume pinning force is given by the relationship $F_p(B) = B \cdot J_c(B)$. Using this expression, the reduced volume pinning force, $f = F_p(B)/F_{p\,max}$, as a function of reduced magnetic field $b = B/B^*$ can be plotted from the magnetization data. The resulting graph is depicted in figure 6, along with the curves (shown as solid lines) best fitting on various data sets obtained from $f \propto b^p(1-b)^q$, using different values for p and q (collected in table 3). The well-known values for the classical FLS model are $p = 0.5$ and $q = 2$ [17, 20, 21].

Although the value of $p \approx 0.5$ for all the samples of set 1, $q \approx 2.0$ only for the pristine sample and for the one irradiated with 1×10^{12} Au ions cm^{-2}. This indicates that the flux pinning in these two samples is primarily governed by the classical FLS mechanism, which takes into account similar channels with identical properties only [17, 20, 21]. The curves corresponding to the sample irradiated with 5×10^{10} Au ions cm^{-2} have $q \ll 2.0$, suggesting the possibility of additional core pinning due to nano-scale precipitates [21] that may be present in this particular sample. Interestingly, for $b > 6.0$, both the irradiated samples of set 1 show a variation towards higher f values at both temperatures, even with the values of p and q as given in table 3, which fit most of the data points for $b < 6.0$. Two inferences may be derived from these observations. First, within the framework of the FLS model, such deviations at higher fields point to a variation in the FLS channel width and its superconducting properties. Hence, identical FLS channels cannot be held responsible for the observed properties. It has also been reported that a change in temperature and heavy-ion irradiation can result in the distribution of channel widths and its superconducting properties [17]. Second, the shift of the data points towards higher F_p values is essentially an indication of the higher pinning efficiency

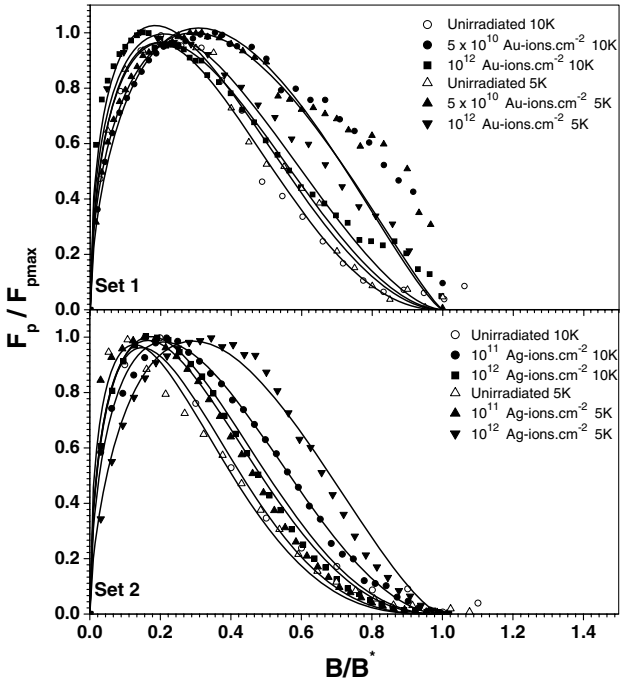

Figure 6. Reduced volume pinning force as a function of reduced field at two different temperatures for both sets of samples. Solid lines show the best-fitting theoretical curves for each data-set, using the expression $f = Ab^p(1-b)^q$. The various values of p and q are given in table 3.

Table 3. Values of p and q for the best fit curves of figure 6.

Set, T	Sample	p	q
Set 1, 5 K	Pristine	0.55	2.2
	5×10^{10} Au ions cm^{-2}	0.58	1.3
	10^{12} Au ions cm^{-2}	0.45	2.0
Set 1, 10 K	Pristine	0.50	1.9
	5×10^{10} Au ions cm^{-2}	0.50	1.2
	10^{12} Au ions cm^{-2}	0.45	1.7
Set 2, 5 K	Pristine	0.52	3.0
	10^{11} Ag ions cm^{-2}	0.53	2.0
	10^{12} Ag ions cm^{-2}	0.50	2.4
Set 2, 10 K	Pristine	0.46	3.1
	10^{11} Ag ions cm^{-2}	0.49	2.4
	10^{12} Ag ions cm^{-2}	0.59	1.7

of the Au-ion-irradiated samples, which is an observation that satisfactorily explains the higher enhancement of J_c in these samples compared to those irradiated with Ag ions. In this scenario, however, the possibility of the existence of other pinning mechanisms in the Au-ion-irradiated samples, beside the flux shear, cannot be ruled out. On the other hand, for set 2, the classical FLS mechanism seems to hold for all the samples, as p and q have values of around 0.5 and 2.0, respectively. Only for the pristine sample of this set the value of q (≈ 3) is slightly higher. Nevertheless, since almost all the data points of this set seem to retain the bell shape of the

theoretical curve, it can be concluded that the FLS is the dominant mechanism of pinning throughout the range of B values considered for this set.

4. Conclusion

We have studied the effect of 200 MeV Au and 200 MeV Ag ion irradiation on the temperature and field dependences of the critical current density J_c of MgB_2 thin films on sapphire substrate. Two films were irradiated with 5×10^{10} and 1×10^{12} Au ions cm^{-2}, and two films with 1×10^{11} and 1×10^{12} Ag ions cm^{-2}, respectively. After irradiation, the critical temperature T_c decreased for all samples except for the one with a higher dose of gold ions, where it increased marginally. These observations were also confirmed from the measurements of normalized magnetization as a function of temperature with a constant applied field of 10^{-2} T. The degradation of T_c is an expected result, as the grain connectivity of the samples usually decreases after irradiation. However, the marginal post-irradiation increase in T_c in one of the samples is somewhat curious, which may be due to irradiation-induced atomic rearrangements, leading to the formation of regions with better grain connectivity. This atomic rearrangement is evident in the SEM results too. Moreover, the small fluctuations observed in the $R(T)$ curves for Au-ion-irradiated samples may also be explained by a similar argument, i.e. irradiation introduces regions with $R(T)$ properties that are slightly different from the rest of the host. The critical current density J_c for all the samples, estimated from the widths of magnetization loops using Bean's critical state model, was found to increase after irradiation. But the enhancement was more pronounced for the Au ion irradiation. For the pristine as well as the irradiated samples, J_c decreases as expected with increasing temperature and applied magnetic field. The greater enhancement of J_c after Au ion irradiation compared to that after Ag ion irradiation may be explained reasonably within the framework of the FLS model. In the Ag-ion-irradiated samples, the nature of the J_c enhancement seems to agree with the classical FLS model throughout the range of applied magnetic fields considered. However, in the case of Au-ion-irradiated samples, a deviation from the theory at higher magnetic fields indicates a variation in the FLS channel widths and their superconducting properties. These variations probably support higher flux pinning in the Au-ion-irradiated samples compared to those irradiated with Ag ions, and therefore the observed J_c enhancement is higher in the former than in the latter.

Acknowledgments

The work was carried out in part at the Inter University Accelerator Centre (IUAC), New Delhi, India, the National Physical Laboratory (NPL), New Delhi, India and the Indian Institute of Technology, Kanpur (IITK), India. We are grateful to Dr D Kanjilal and the staff at the Pelletron Group (IUAC, New Delhi, India) for the irradiation experiments. One of us (HK, NPL) acknowledges UGC, India for the financial support for the NPL and Indian Universities Superconductivity Collaboration.

References

[1] Nagamatsu J, Nakagawa N, Muranaka T, Zanitani Y and Akimitsu J 2001 *Nature* **410** 63
[2] Buzea C and Yamashita T 2001 *Supercond. Sci. Technol.* **14** R115
[3] Samanta S B, Narayan H, Gupta A, Narlikar A V, Muranaka T and Akimitsu J 2002 *Phys. Rev.* B **65** 092510
[4] Bugoslavsky Y, Cohen L F, Perkins G K, Polichetti M, Tete T J, Gwilliam R and Caplin A D 2001 *Nature* **411** 561
[5] Okayasu S, Ikeda H and Yoshizaki R 2002 *Physica* C **378** 462

[6] Pallecchi I *et al* 2005 *Phys. Rev.* B **72** 184512
[7] Gandikota R *et al* 2005 *Appl. Phys. Lett.* **86** 012508
[8] Narayan H, Samanta S B, Gupta A, Narlikar A V, Kishore R, Sood K N, Kanjilal D, Muranaka T and Akimitsu J 2002 *Physica* C **377** 1
[9] Narayan H, Gupta A, Narlikar A V, Sood K N, Kishore R and Kanjilal D 2004 *Supercond. Sci. Technol.* **17** 1072
[10] Shinde S R *et al* 2004 *Appl. Phys. Lett.* **84** 2352
[11] Kaushik S D, Ravi Kumar, Mishra P K, Geincke J E, Eom C B and Patnaik S 2005 *Preprint* cond-mat/0509755
[12] Chikumoto N, Yamamoto A, Konczykowski M and Murakami M 2003 *Physica* C **388/389** 167
[13] Olsson R J, Kwok W-K, Karapetrov G, Iavarone M, Claus H, Peterson C and Crabtree G W 2002 *Preprint* cond-mat/0201022
[14] Zeng X H *et al* 2003 *Appl. Phys. Lett.* **82** 2097
[15] Ziegler J F and Biersack J P 1997 *Stopping and Range of Ions in Matter, version: 97.09. The Stopping and Range of Ions in Solids* (New York: Pergamon) (for further information and download see: http://www.research.ibm.com/ionbeams/home.htm)
[16] Rowell J M 2003 *Supercond. Sci. Technol.* **16** R17
[17] Gupta A, Narayan H, Astill D, Kanjilal D, Ferdeghini C, Paranthaman M and Narlikar A V 2003 *Supercond. Sci. Technol.* **16** 951
[18] Bean C P 1962 *Phys. Rev. Lett.* **8** 250
[19] Choi E-M, Gupta S K, Sen S, Lee H S, Kim H-J and Lee S-I 2004 *Supercond. Sci. Technol.* **17** S524–7
Kim H-J *et al* 2001 *Phys. Rev. Lett.* **87** 087002
[20] Kramer E J 1980 *J. Appl. Phys.* **51** 4930
[21] Cooley L, Song X and Larbalestier D 2003 *IEEE Trans. Supercond.* **13** 3280